Polyhedron 27 (2008) 3020–3028

Contents lists available at ScienceDirect

Polyhedron

journal homepage: www.elsevier.com/locate/poly

Ruthenium–carbonyl complexes of 1-alkyl-2-(arylazo)imidazoles: Synthesis, structure, spectra and redox properties

T.K. Mondal [a], S.K. Sarker [a], P. Raghavaiah [b], C. Sinha [a,*]

[a] Department of Chemistry, Inorganic Chemistry Section, Jadavpur University, Kolkata 700 032, West Bengal, India
[b] School of Chemistry, National Single Crystal X-ray Diffractometer Facility, University of Hyderabad, Hyderabad 500 046, India

ARTICLE INFO

Article history:
Received 10 April 2008
Accepted 3 June 2008

Keywords:
Azoimidazoles
Ruthenium–carbonyl
X-ray structure
Electrochemistry
DFT calculation

ABSTRACT

trans-(Cl)-[Ru(CO)$_2$Cl$_2$(PaiR/TaiR)] compounds have been synthesized by reacting 1-alkyl-2-(phenylazo)imidazole (PaiR) or 1-alkyl-2-(*p*-tolylazo)imidazoles (TaiR) with [Ru(CO)$_2$Cl$_2$]$_n$ in methanol under refluxing conditions. The X-ray crystallographic study of *trans*-(Cl)-[Ru(CO)$_2$Cl$_2$(PaiEt)] (PaiEt = 1-ethyl-2-(phenylazo)imidazole) shows a distorted octahedral geometry with a *trans*-Cl,Cl configuration. An intermolecular hydrogen bonded dimer serves as a motif in the supramolecular network with C–H$\cdots\pi$ and $\pi\cdots\pi$ interactions. The complexes show metal oxidation, Ru(III)/Ru(II); and reduction of the coordinated azo (–N=N–) function. The molecular orbital diagram has been drawn by density functional theory (DFT) using an optimized geometry from the single crystal X-ray parameters. The electronic movement and assignment of electronic spectra have been carried out by TD-DFT calculations both in the gas and acetonitrile phase.

1. Introduction

The tremendous development of the coordination chemistry of 2,2-bipyridine and its applications [1–4] have inspired the design of N,N-donor ligands in which one of the donor centers comes from pyridine or a *N*-heterocycle. Ligands consisting of one *N*-heterocyclic ring with a conjugated pendant azo (–N=N–) group at the *ortho*-position give an azoimine (–N=N–C=N–) linkage, isoelectronic with the diimine function (–N=C–C=N–), and serve as an efficient π-acidic ligand [5–40]. The high π-acceptance ability of the azo-N participates through the π*-azo orbital. Consequently, the ligands are able to stabilize metal ions in their lower oxidation states. Examples are 2-(arylazo)pyridines, whose ruthenium(II) compounds have been reported in recent years [48–52,12,53–58] with reference to the exploration of their structural diversity, electrochemical properties, catalytic and anticancer activities.

Ruthenium and osmium carbonyl complexes of azopyridines act as a CO reservoir and may be used for hydroformylation or other CO insertion reactions [30–44,6,45,7,46,47]. In organic transformations these metal carbonyls play a crucial role [1–4,41–44,6,45,7,46,47]. Carbonyl–ruthenium(II) polypyridine complexes are excellent catalysts and catalyst precursors for the reduction of CO_2 or the water gas shift reaction [59–61]. They are used as building blocks for making organometallic-based nanostructures *e.g.*, Ru-wire polymeric materials, [Ru(bpy)(CO)$_2$]$_n$ [62]. Among these, [Ru(CO)$_2$Cl$_2$(bpy)] is the main precursor [63,64]. This has prompted us to undertake a study of Ru–carbonyl complexes of azoheterocycles.

We have been engaged for the last few years in the design of azoimidazole molecules [18–29]. Imidazole and its derivatives were chosen because of their chemical and biological ubiquity [65], whilst the azo group enhances π-acidity and is responsible for photochromism [66–68], pH-responsive and redox activity in the molecules [26–44,6,45,7,46–52,12,53–58].

In this work, we report on the reaction of 1-alkyl-2-(arylazo)imidazole [1-alkyl-2-(phenylazo)imidazoles (PaiR, **1**) and 1-alkyl-2-(*p*-tolylazo)imidazoles (TaiR, **2**)] with [Ru(CO)$_2$Cl$_2$]$_n$. The products are characterized by microanalytical and spectroscopic data which support the composition, [Ru(CO)$_2$Cl$_2$(PaiR)] (**3**) and [Ru(CO)$_2$Cl$_2$(TaiR)] (**4**). The electronic structures of [Ru(CO)$_2$Cl$_2$(PaiEt)] (**3b**) and [Ru(CO)Cl$_2$(PaiEt)(NCMe)] (**5b**) have been calculated by DFT and TD-DFT methods. The calculated information has been used to rationalize the electronic spectra and redox properties of the complexes:

$$[Ru(CO)_2Cl_2]_n + N,N' \xrightarrow{Reflux,MeOH} \textit{trans}\text{-}(Cl)\text{-}[Ru(CO)_2Cl_2(N,N')] \quad (1)$$

$$\textit{trans}\text{-}(Cl)\text{-}[Ru(CO)_2Cl_2(N,N')] + Me_3NO \xrightarrow{Reflux,MeCN} \textit{trans}\text{-}(Cl)\text{-}[Ru(CO)Cl_2(N,N')(MeCN)] \quad (2)$$

* Corresponding author. Fax: +91 033 2413 7121.
E-mail address: c_r_sinha@yahoo.com (C. Sinha).

0277-5387/$ - see front matter © 2008 Published by Elsevier Ltd.
doi:10.1016/j.poly.2008.06.027

2. Results and discussion

2.1. Synthesis and formulation

Reaction of $[Ru(CO)_2Cl_2]_n$ as a methanol suspension with 1-alkyl-2-(phenylazo)imidazole (PaiR) (**1**) or 1-alkyl-2-(*p*-tolylazo)-imidazole (TaiR) (**2**) (where R = Me (**a**), CH_2CH_3 (**b**), CH_2Ph (**c**)) under refluxing conditions in a dinitrogen atmosphere resulted in a brown solution Eq. (1). Upon slow evaporation of the solvent a brown crystalline product was left. The formulation of the complexes, $[Ru(CO)_2Cl_2(PaiR)]$ (**3**) and $[Ru(CO)_2Cl_2(TaiR)]$ (**4**) have been supported by microanalytical data (Section 4). Although three geometrical isomers (**3** and **4**; **3′** and **4′**; **3″** and **4″**) are possible, we have isolated only one isomer, with the CO groups *cis* to each other (**3** and **4**) and two Cl ligands in a *trans* disposition (Scheme 1). The complexes are diamagnetic, indicating the presence of the metal in the +2 oxidation state (d^6). Three stereo-isomers of **3**/**4**, **3′**/**4′** and **3″**/**4″** are possible. The structure has been established by a single crystal X-ray diffraction study in the case of $[Ru(CO)_2Cl_2(PaiEt)]$ and has a *trans*-(Cl,Cl) geometry, abbreviated as *trans*-(Cl)-$[Ru(CO)_2Cl_2(PaiR/TaiR)]$ (**3** or **4**). The higher stability of the *trans*-(Cl)-*cis*-(CO) isomer relative to the *cis*-(Cl)-*trans*-(CO) isomer is not surprising due to the *trans* weakening effect of CO. The selectivity of the *trans*-(Cl) configuration has also been supported by DFT calculations (*vide Section* 2.3). Complexes **3** and **4** undergo a selective mono-decarbonylation reaction upon refluxing with Me_3NO in acetonitrile Eq. (2). In this process one CO is released and MeCN is coordinated, *trans*-(Cl)-$[Ru(CO)Cl_2(PaiR)(NCMe)]$ (**5**) and *trans*-(Cl)-$[Ru(CO)Cl_2(TaiR)(NCMe)]$ (**6**) are formed. The structure of the mono-carbonylated product (**5**, **6**) is supported by a single stretch ν (CO) in the FT-IR spectra (Fig. 1), elemental analysis and ^1H NMR spectroscopic measurements. Although isomerisation to give *cis*-(Cl)-$[Ru(CO)Cl_2(ligand)(NCMe)]$ is possible, we cannot establish the presence of this isomer, even in the mixed form. The photochemical treatment of the precursor was also unsuccessful for isomerisation and giving the full decarbonylated complexes. The crystals of these complexes are weakly diffracting for X-ray structure determination. The full removal of CO has not been achieved even under drastic reaction conditions in the presence of a large excess of Me_3NO [69,70]. This reaction yielded an intractable brown solid.

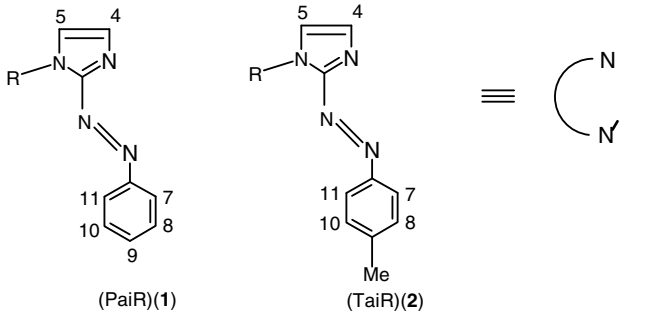

Scheme 1.

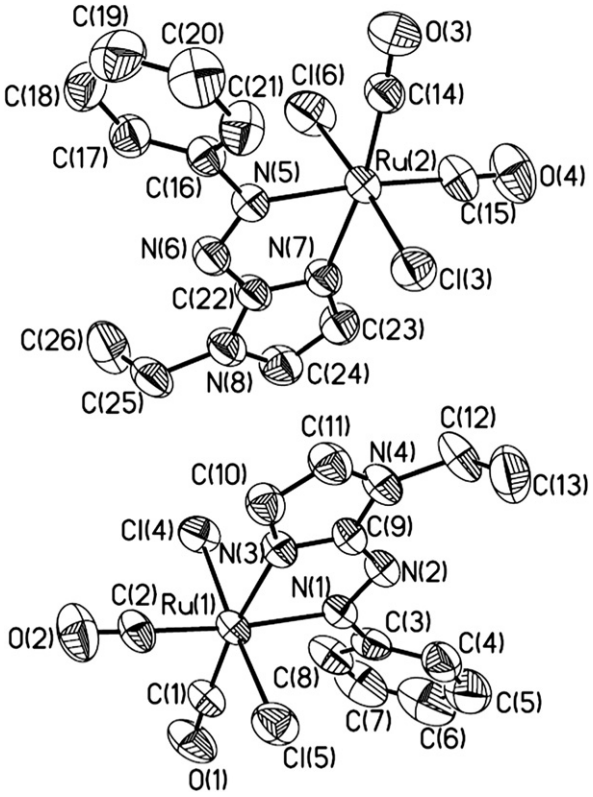

Fig. 1. Molecular structure of two conformers of *trans*-(Cl)-$[Ru(CO)_2Cl_2(PaiEt)]$ (**3b**) (30% probability ellipsoids).

2.2. Molecular structure

The X-ray structure of $[Ru(CO)_2Cl_2(PaiEt)]$ (**3b**) is shown in Fig. 1; selected bond parameters are listed in Table 1. The ligands dispositions determine the structure as *trans*-(Cl)-$[Ru(CO)_2Cl_2(PaiEt)]$. The molecule consists of a central Ru surrounded by six donor centers, and the arrangement is distorted octahedral. The atomic arrangement involves two *trans*-chlorine, two *cis*-CO and a chelated 1-ethyl-2-(phenylazo)imidazole (PaiEt) ligand within the $RuCl_2C_2N_2$ coordination sphere. The two CO ligands are *trans* to the azo-N and imidazole-N coordinated centers. The asymmetric unit of the lattice consists of two molecules. A view of the diad, including the atomic numbering scheme, is given in Fig. 1. In terms of bond distances and angles, as well as gross geometry, the two molecules are closely alike to one another. The chelate ring dimensions (∠N(3)–Ru(1)–N(1): 75.13(9) and ∠N(5)–Ru(2)–N(7): 75.28(9)) are comparable with those in other structurally characterized chelates of the azoimine function [26–29,41–44,6,45,7,46–52,12,53–58]. The *trans* chlorine angles, Cl(4)–Ru(1)–Cl(5), 177.14(3) and Cl(3)–Ru(2)–Cl(6), 176.04(3), lie in the range of reported data [51,52,12,53–58]. Other angles about Ru define the distorted octahedral geometry.

The Ru–N(azo) distance (Ru(1)–N(1), 2.132(2); Ru(2)–N(5), 2.123(2) Å) is slightly longer than Ru–N(imidazole) (Ru(1)–N(3), 2.102(2); Ru(2)–N(7), 2.106(2) Å). In general, the Ru–N(azo) bond distance is shorter than the Ru–N(imidazole) bond, which is mainly due to $d\pi(Ru) \rightarrow \pi^*(azo)$ back bonding [26–44,6,45,7,46–48]. The –N=N– bond length is 1.275–1.279 Å and is longer than the free ligand azo distance (1.258 Å) [66–68], which supports the $d\pi(Ru)$–$\pi^*(azo)$ back bonding. Of the Ru–C bond lengths, (Ru(1)–C(1), 1.879(3); Ru(1)–C(2), 1.894(3); Ru(2)–C(14), 1.876(3); Ru(2)–C(15), 1.894(3) Å) the bonds *trans* to Ru–N(imidazole) (Ru(1)–C(1) and Ru(2)–C(14)) are shorter than the bonds

Table 1
Selected bond distances (Å) and bond angles (°) of (**3b**), X-ray and theoretical

Molecule-1		Molecule-2		Calculated structure
C(1)–O(1)	1.133(4)	C(14)–O(3)	1.130(4)	1.139
C(2)–O(2)	1.116(4)	C(15)–O(4)	1.113(4)	1.122
Ru(1)–C(1)	1.879(3)	Ru(2)–C(14)	1.876(3)	1.884
Ru(1)–C(2)	1.894(3)	Ru(2)–C(15)	1.894(3)	1.906
Ru(1)–N(1)	2.132(2)	Ru(2)–N(5)	2.123(2)	2.138
Ru(1)–N(3)	2.102(2)	Ru(2)–N(7)	2.106(2)	2.112
Ru(1)–Cl(4)	2.3798(8)	Ru(2)–Cl(3)	2.3823(8)	2.394
Ru(1)–Cl(5)	2.3852(9)	Ru(2)–Cl(6)	2.3799(9)	2.390
N(1)–N(2)	1.279(3)	N(5)–N(6)	1.275(3)	1.288
O(1)–C(1)–Ru(1)	177.6(3)	O(3)–C(14)–Ru(2)	176.0(3)	178.1
O(2)–C(2)–Ru(1)	177.9(3)	O(4)–C(15)–Ru(2)	178.9(3)	178.2
C(1)–Ru(1)–C(2)	88.34(12)	C(14)–Ru(2)–C(15)	89.08(14)	90.21
C(1)–Ru(1)–N(3)	172.53(12)	C(14)–Ru(2)–N(7)	171.38(12)	174.1
C(2)–Ru(1)–N(3)	98.53(11)	C(15)–Ru(2)–N(7)	98.51(11)	95.06
C(1)–Ru(1)–N(1)	98.13(11)	C(14)–Ru(2)–N(5)	97.11(11)	98.70
C(2)–Ru(1)–N(1)	173.53(11)	C(15)–Ru(2)–N(5)	173.79(11)	170.9
C(1)–Ru(1)–Cl(4)	93.37(10)	C(14)–Ru(2)–Cl(3)	94.00(10)	92.42
C(2)–Ru(1)–Cl(4)	89.77(11)	C(15)–Ru(2)–Cl(3)	90.64(11)	91.64
C(1)–Ru(1)–Cl(5)	88.98(10)	C(14)–Ru(2)–Cl(6)	89.40(10)	89.92
C(2)–Ru(1)–Cl(5)	91.94(11)	C(15)–Ru(2)–Cl(6)	91.44(11)	91.80
N(3)–Ru(1)–N(1)	75.13(9)	N(7)–Ru(2)–N(5)	75.28(9)	75.93
N(1)–Ru(1)–Cl(4)	87.69(7)	N(7)–Ru(2)–Cl(6)	86.35(7)	89.67
N(3)–Ru(1)–Cl(4)	89.61(7)	N(5)–Ru(2)–Cl(6)	88.14(7)	89.88
N(1)–Ru(1)–Cl(5)	90.35(7)	N(7)–Ru(2)–Cl(3)	90.01(7)	86.55
N(3)–Ru(1)–Cl(5)	87.87(7)	N(5)–Ru(2)–Cl(3)	89.43(7)	87.47

that are *trans* to Ru–N(azo) (Ru(1)–C(2) and Ru(2)–C(15)). This is usual due to a better *trans influence* of imidazole-N compared to azo-N donors. The C–O distances (C(1)–O(1), 1.133(4); C(2)–O(2), 1.116(4); C(14)–O(3), 1.130(4); C(15)–O(4), 1.113(4) Å) vary to within 0.01–0.02 Å. The difference between the two molecules in the lattice primarily lies in the detail of the conformation. The pendant phenyl ring is inclined to the mean plane of the chelate ring, and the angles are molecule-1, 36.73(17); molecule-2, 41.99(15). The torsion angles vary in a characteristic manner. Examples from those among the atoms of the chelate ring are: Ru(1)–N(3)–C(9)–N(2): 2.2(4); Ru(2)–N(7)–C(22)–N(6): −3.3(4); C(9)–N(2)–N(1)–Ru(1): −1.3(3); C(22)–N(6)–N(5)–Ru(2): 2.4(3); N(2)–N(1)–Ru(1)–N(3): 1.8(2); N(6)–N(5)–Ru(2)–N(7): −3.2(2). Thus, these two molecules represent a subtle form of conformational isomerism in a metal chelate, sustained by the crystal lattice.

Non-covalent interactions, C–H$\cdots\pi$ and $\pi\cdots\pi$, exist to provide rigidity to the supramolecule. An intermolecular hydrogen bond between one of the coordinated Cl ligands and the H atom of the *ortho* C–H of the pendant azophenyl group of an adjacent molecule constitutes a dimer structure (Fig. 2a). Each dimer interacts with adjacent dimers *via* C–H$\cdots\pi$ and $\pi\cdots\pi$ interactions to generate a supramolecular network (Fig. 2b). The interactions are summarized in Table 2.

2.3. DFT and TD-DFT calculations

DFT and TD-DFT calculations were performed for complexes **3b** and **5b**. All the calculations were performed using the GAUSSIAN03 (G03) [71] software package, running under Windows. The Becke's three-parameter hybrid exchange functional and the Lee–Yang–Parr non-local correlation functional [72] (B3LYP) was used throughout. Elements except ruthenium were assigned a 6-31 G* basis set in our calculations. For ruthenium the Los Alamos effective core potential plus double zeta (LanL2DZ) [73] basis set was employed. Gas and solution-phase geometry optimization was carried out. In all cases, vibrational frequencies were calculated to ensure that the optimized geometries represented local minima. To check the effect of solvation on the calculated optical absorption spectra, we performed TD-DFT calculations of the low lying excitation at the singlet optimized geometry, including the solvation effect by means of the non-equilibrium implementation of the polarizable continuum model [74]; as in the experimental conditions, the chosen solvent was acetonitrile. GaussSum [75] was used to calculate the fractional contributions of various groups to each molecular orbital. This is done using Mulliken population analysis.

The calculated structure of **3b** correlates very well with the results of its X-ray analysis (Fig. 1, Table 1). The theoretical Ru–N bond lengths are about 0.010 Å longer than those observed. Similarly the experimental Ru–Cl distances are shorter by 0.015 Å than the theoretical data. The Ru–C and C–O distances are also reduced by 0.006–0.010 Å in the experimental data compared to the calculated structure. The computation of ν(CO) from the DFT calculation shows a lowering of frequency by 8–10 cm^{-1}.

The DFT calculation shows a lower energy of the HOMO of *trans*-(Cl)-[$Ru(CO)_2Cl_2$(PaiEt)] (**3b**) (E_{HOMO}): −6.17 eV) than that of *cis*-(Cl)-[$Ru(CO)_2Cl_2$(PaiEt)] (**3b′**) (E_{HOMO}): −5.60 eV) and *cis*-(Cl)-*cis*-(CO)-[$Ru(CO)_2Cl_2$(PaiEt)] (**3b″**) (E_{HOMO}): −5.86 eV). This reflects better stability of the *trans*-(Cl,Cl) than *cis*-(Cl,Cl) configuration. An interesting feature of the valence orbitals is that the highest occupied MOs (HOMO, abbreviated as H, H − 1, H − 2, H − 3) contain >65% and >45% of the Cl atomic functions in **3b** and **5b**, respectively. Metal orbitals contribute >20% to H and H − 1. The LUMO (abbreviated L) is mostly characterized by the azoimidazole ligand function (>80%) for both these complexes, while other unoccupied molecular orbitals have CO >20% and Ru contribution varies from 5% to 35%. The results in acetonitrile phase show a significant difference from the gas phase, in particular to the occupied MOs. In the HOMO the contribution of PaiEt (L) is 42% in MeCN and 1% in the gas phase, while the Cl contribution is 28% in MeCN and the gas phase contribution is 67% for **3b**. The situation is different for **5b**: 14% (gas) and 24% (MeCN). H − 1 in the gas and acetonitrile phases remains more or less the same. The HOMO is stabilized by 0.63 eV in **3b** and 0.72 eV in **5b** from the gas to acetonitrile phase. The HOMO is also lowered in energy by 0.54 eV in **3b** compared to **5b** and the HOMO–LUMO energy gaps are 3.04 eV for **3b** and 2.83 eV for **5b** in MeCN (Fig. 3).

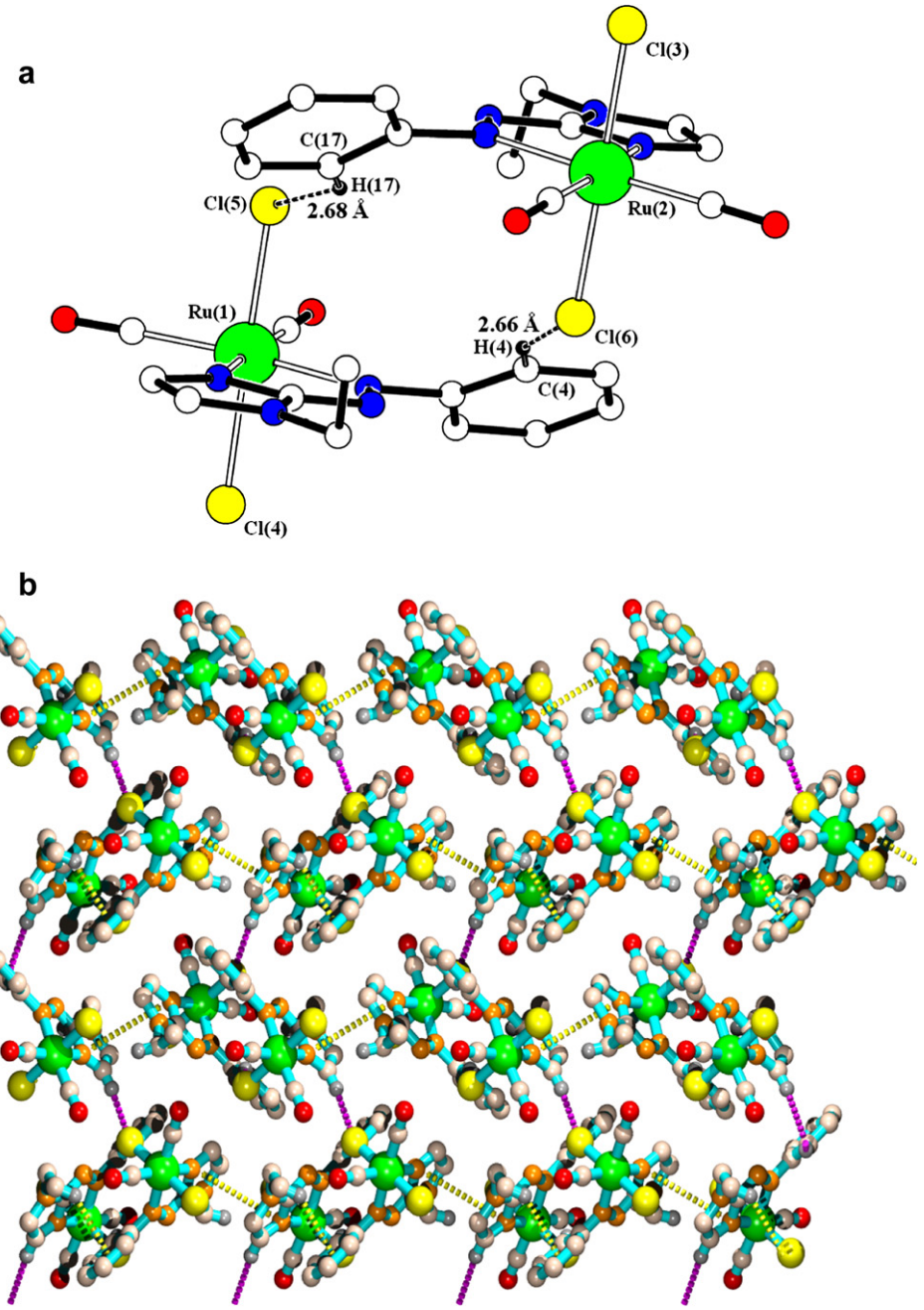

Fig. 2. (a) C–H···Cl hydrogen bonded dimer unit, (b) π···π and CH···π interacted *ab*-plane (π···π; C–H···π in yellow; C–H···Cl in magenta). (For interpretation of the references to color in this figure legend, the reader is referred to the web version of this article.)

Table 2
Distance of non-covalent interactions in **3b**

	d_{C-H} (Å)	$d_{H\cdots Cl}$ (Å)	$d_{C\cdots Cl}$ (Å)	Angle (°)	Symmetry
Hydrogen bonding					
C(4)–H(4)···Cl(6)	0.930	2.680	3.560(4)	157.0	$-1+x, y, z$
C(17)–H(17)···Cl(5)	0.930	2.660	3.456(3)	144.0	$1+x, y, z$
	$d_{H\cdots Cg}$ (Å)	d_{C-Cg} (Å)	Angle (°)	Symmetry	
C–H···π interaction					
C(13)–H(13 C) → Cg(3)	2.984	3.799(8)	143.45	$-1+x, y, z$	
	$d_{Cg\cdots Cg}$ (Å)	Alpha	*d* (perpendicular)	Symmetry	
π···π interaction					
Cg(2) → Cg(5)	3.691(2)	1.02	3.447	x, y, z	

Cg(2): N(7)–C(22)–N(8)–C(24)–C(23); Cg(3): C(16)–C(17)–C(18)–C(19)–C(20)–C(21); Cg(5): N(3)–C(9)–N(4)–C(11)–C(10).

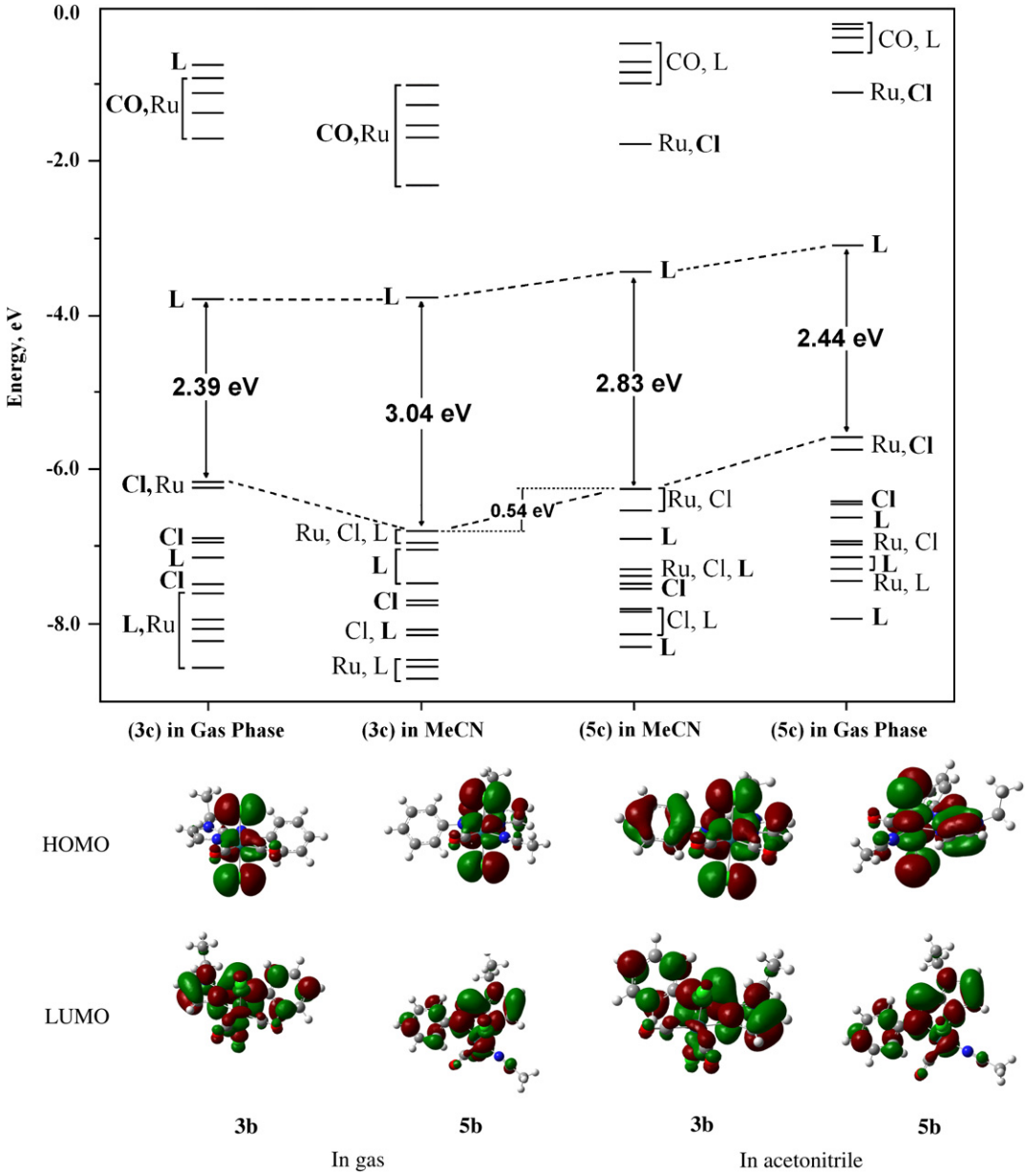

Fig. 3. Energy level correlation diagram of **3b** and **5b** in the gas and acetonitrile phase (top) and HOMO, LUMO picture (bottom).

2.4. Spectra and bonding

The infrared spectra of **3** and **4** show the presence ν (CO) stretching vibrations at 1990–2010 and 2065–2075 cm^{-1} (Table 3) which indicates the *cis* coordination of two CO ligands [67–70,76–78] (Fig. 1.) ν(Ru–Cl) appears at 330–340 cm^{-1}. Other significant peaks appear at 1570–1590 cm^{-1} and 1350–1370 cm^{-1}, corresponding to ν(C=N) and ν(N=N), respectively. The azo stretching is significantly shifted to the lower frequency region compared to the free ligand value (1400–1410 cm^{-1}) [79,80], which supports an efficient back donation, $d\pi(Ru(II)) \rightarrow \pi^*(azo)$. The infrared spectra of **5** and **6** show one ν(CO) at 1980–1985 cm^{-1}, which is in support of mono-carbonyl formulation, and the shifting to the lower frequency region compared to ν(CO) of **3/4** is an indication of better $d\pi(Ru(II)) \rightarrow \pi^*(CO)$ donation in **5/6**. The Mulliken population analysis of **3b** and **5b** show that the positive charge on CO in **5b** (0.18619) is less than that of the CO groups in **3b** (0.21986 and 0.23749). Computation of the major frequencies, ν(C=N), ν(N=N), ν(CO) and ν(Ru–Cl), by the DFT calculation shows a slightly lower frequency (5–10 cm^{-1}) than that of the experimental data, but still being within the reported frequency range.

The electronic spectra of **3** and **4** show an intense broad band at 470–500 nm, and in addition to this the molecules show a more intense and sharp band at 380–400 nm. The lower energy band in the mono-carbonyl complexes (**5** and **6**) has been shifted to a longer wavelength by 15–20 nm compared to the di-carbonyl precursors, **3** and **4** (Fig. 4). Thus, the energy of transition is lowered in **5/6** compared to **3/4**. This is well explained on the basis of the DFT calculation using the optimized geometry of a representative complex. The DFT calculations of **3b** and **5b** show that the HOMO–LUMO energy gap decreased by 0.21 eV in **5b** compared to **3b** in acetonitrile (Fig. 3). The TD-DFT calculations of **3b** and **5b** show that the transition at 470–530 nm (Table 5) could be assigned to $H/H-1 \rightarrow L$. H and H − 1 are localized on parts of the metal and Cl, and L have major ligand character. Thus, the transition is admix-

Table 3
FT-IR[a], UV–Vis spectral[b] and cyclic voltammetric[c] data of the complexes

Complex	IR data ν(CO) (cm^{-1})[a]	UV–Vis spectral data[b] λ_{max} (nm) ($10^{-3} \in M^{-1} cm^{-1}$)	Cyclic voltammetric data[c]	
			$E_{Ru(III)/Ru(II)}$, V (ΔE_p, mV)	Ligand reduction, V (ΔE_p, mV)
trans-(Cl)-[Ru(CO)$_2$Cl$_2$(PaiMe)] (**3a**)	1995, 2068	388(13.76), 500(3.07)	1.35(130)	−0.46(120), −1.30(210)
trans-(Cl)-[Ru(CO)$_2$Cl$_2$(PaiEt)] (**3b**)	2010, 2072	399(12.43), 480(2.88)	1.30(130)	−0.48(120), −1.32(210)
trans-(Cl)-[Ru(CO)$_2$Cl$_2$(PaiBz)] (**3c**)	2000, 2070	390(12.83), 498(3.05)	1.40(140)	−0.50(120), −1.30(210)
trans-(Cl)-[Ru(CO)$_2$Cl$_2$(TaiMe)] (**4a**)	2000, 2068	392(12.84), 498(2.37)	1.36(140)	−0.48(120), −1.25(210)
trans-(Cl)-[Ru(CO)$_2$Cl$_2$(TaiEt)] (**4b**)	2003, 2070	395(13.64), 500(2.82)	1.30(130)	−0.55(120), −1.30(210)
trans-(Cl)-[Ru(CO)$_2$Cl$_2$(TaiBz)] (**4c**)	1990, 2068	390(11.49), 505(2.73)	1.35(140)	−0.53(120), −1.35(210)
trans-(Cl)-[Ru(CO)Cl$_2$(PaiMe)(NCMe)] (**5a**)	1975	369(11.28), 540(3.24)	0.82(110)	−0.53(125), −1.25(220)
trans-(Cl)-[Ru(CO)Cl$_2$(PaiEt)(NCMe)] (**5b**)	1980	386(12.50), 515(2.92)	0.84(110)	−0.58(130), −1.28(220)
trans-(Cl)-[Ru(CO)Cl$_2$(PaiBz)(NCMe)] (**5c**)	1970	382(10.64), 530(4.65)	0.85(110)	−0.60(120), −1.26(220)
trans-(Cl)-[Ru(CO)Cl$_2$(TaiMe)(NCMe)] (**6a**)	1972	383(11.34), 530(3.21)	0.80(110)	−0.57(120), −1.26(220)
trans-(Cl)-[Ru(CO)Cl$_2$(TaiEt)(NCMe)] (**6b**)	1982	383(10.84), 530(4.68)	0.85(100)	−0.62(125), −1.30(220)
trans-(Cl)-[Ru(CO)Cl$_2$(TaiBz)(NCMe)] (**6c**)	1968	378(11.33), 525(2.94)	0.87(100)	−0.65(120), −1.27(220)

[a] KBr disc.
[b] Solvent, dry acetonitrile.
[c] Solvent MeCN, Pt-disk working electrode, Ag/AgCl reference electrode, Pt-wire auxiliary electrode, [nBu$_4$N][ClO$_4$] supporting electrolyte. $E_{Ru(III)/Ru(II)} = 0.5(E_{pa} + E_{pc})$, V for Ru(III)/Ru(II) couple in unit of V, $\Delta E_p = E_{pa} - E_{pc}$, mV where E_{pc} (cathodic-peak-potential), E_{pa} (anodic-peak-potential).

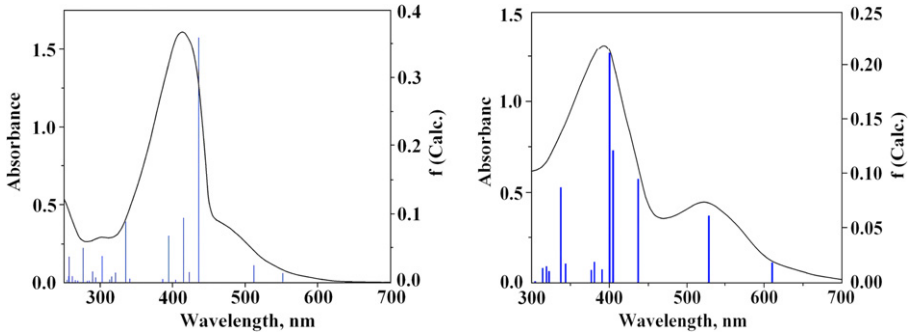

Fig. 4. Experimental UV–Vis spectra and calculated transitions for **3b** (left) and **5b** (right) in acetonitrile.

ture of MLCT and XLCT transitions (X = Cl) [81]. Because of the Cl contribution to H − n (n = 2, 3, 4, 5) (40–80%), the H − n → L transitions may be attributed to XLCT and contribute to the broadening of the band. The transitions H/H − n (n = 1–5) → L + p (p = 1, 2, 3, etc.) may be explained as π(PaiEt) → π^*(CO), an inter-ligand charge transfer transition. This transition is also mixed with π (PaiEt) → π^*(PaiEt) transitions.

The imidazole protons (4- and 5-H) of the coordinated PaiR or TaiR in the complexes *trans*-(Cl)-[Ru(CO)$_2$Cl$_2$(PaiR/TaiR)] (**3**, **4**) show downfield shifting by 0.3–0.4 ppm compared to the free ligand data [75–81] and appear at 7.70–7.85 ppm (4-H) and 7.35–7.50 (5-H) ppm (Table 4). This supports the strong preference of the binding of imidazole-N to Ru(II). 1-Me of the coordinated PaiMe/TaiMe in **3a** or **4a** is singlet at 4.25–4.30 ppm; 1-CH$_2$–CH$_3$ of coordinated PaiEt or TaiEt in **3b** or **4b** appears as a quartet at 4.60–4.65 ppm, (J = 8.0 Hz) and a triplet 1.70–1.72 ppm (J = 7.5 Hz) for –CH$_2$– and –CH$_3$, respectively; 1-CH$_2$–(Ph) in (**3c** and **4c**) is singlet at 5.80–5.90 ppm. The mono-carbonyl complexes, **5** and **6**, in general, show aromatic proton signals at a lower chemical shift position (δ) compare to **3** and **4** (with a difference in chemical shift ($\Delta\delta$) of 0.1–0.3 ppm). This may be due to removal of the strongly π-acidic CO from the Ru(CO)$_2$-motif (**3**, **4**) to prepare the Ru(CO)-motif in **5** and **6**. The coordinated MeCN in **5** and **6** appears as a singlet at 2.07-2.15 ppm for δ (CH$_3$).

2.5. Electrochemistry

The complexes show a Ru(III)/Ru(II) couple (Table 3, Fig. 5) when scanned in the potential range 0.0–2.0 V. The response is quasireversible in nature, as is evident from their peak-to-peak separation (ΔE_p > 100 mV). The nature of the voltammogram does not change with the scan rate (50–250 mV s^{-1}). The Ru(III)/Ru(II) potential, *ca.* 1.35 V, of *trans*-(Cl)-[Ru(CO)$_2$Cl$_2$(PaiR/TaiR)] (**3**, **4**) is significantly shifted to *ca.* 0.85 V for *trans*-(Cl)-[Ru(CO)Cl$_2$(PaiR/TaiR)(NCMe)] (**5**, **6**). This may be due to the better electron withdrawing effect of two CO in **3**, **4** than that of one CO in **5**, **6**. The DFT calculation in acetonitrile also supports the lower energy of the HOMO in **3b** (−6.80 eV) compared to that of **5b** (−6.26 eV). The HOMO is also contributed to by the metal (Ru) orbitals, thus the redox response is assigned to the Ru(III)/Ru(II) couple.

On scanning in the negative direction (0 to −2.0 V), two redox responses are observed. The first response is observed at >−0.70 V, and is quasireversible ($\Delta E_p \geqslant 120$ mV) in nature, while the second one appears at <−1.2 V ($\Delta E_p \geqslant 200$ mV). The chelated ligand belongs to the π-acidic azoimine family and can accommodate two electrons centered at the azo group (–N=N–). The reductive responses are assigned to accommodation of electrons in the azo dominated function [–N=N–]/[–N⋯N–]$^-$ and [–N⋯N]$^-$/[–N–N–]$^{2-}$. Ligand reduction of azoimidazole complexes appear at negative potentials and the present data appear at a less negative value (−0.5 to −0.6 V) than that of *trans*-[Ru(ligand)$_2$Cl$_2$] (−0.7 to −0.8 V). The DFT data have assigned that the LUMO of the complexes are constituted mainly of the azo group of the ligand (>80%) and thus the reduction is considered as electron accommodation at the azo dominated orbitals.

3. Conclusion

A series of di-carbonyl complexes of the formulae *trans*-(Cl)-[Ru(CO)$_2$Cl$_2$(PaiR or TaiR)] (for PaiR: R = Me (**3a**), Et (**3b**), CH$_2$Ph

Table 4
^{1}H NMR spectral data of the complexes in $CDCl_3$ at 298 K

Compound	δ, ppm (J, Hz)						
	4-H[a]	5-H[a]	7, 11-H[b]	8, 10-H	9-H/Me	1-R	CH_3CN
3a	7.78	7.44	8.08 (7.5)	7.52[c]	7.52[c]	4.27[e]	
3b	7.82	7.48	8.08 (7.5)	7.62[c]	7.62[c]	4.65 (8.0)[g], 1.70 (7.5)[h]	
3c	7.84	7.50	8.10 (7.5)	7.60[c]	7.60[c]	5.82[f]	
4[a]	7.76	7.44	7.98 (8.0)	7.36[b] (8.0)	2.50[d]	4.30[e]	
4b	7.78	7.45	8.00 (8.0)	7.40[b] (8.0)	2.50[d]	4.62 (8.0)[g], 1.70 (7.5)[h]	
4c	7.78	7.47	8.05 (8.0)	7.42 (7.8)	2.48[d]	5.94[f]	
5[a]	7.61	7.21	7.80 (7.5)	7.42[c]	7.42[c]	4.20[e]	2.06
5b	7.62	7.28	7.85 (7.5)	7.42[c]	7.42[c]	4.60 (7.5)[g], 1.74 (7.5)[h]	2.07
5c	7.65	7.31	7.83 (7.5)	7.50[c]	7.50[c]	5.90[f]	2.06
6a	7.56	7.30	7.68 (8.0)	7.16[b] (8.0)	2.50[d]	4.18[e]	2.06
6b	7.52	7.25	7.70 (8.0)	7.22[b] (7.5)	2.54[d]	4.60 (7.5)[g], 1.75 (7.5)[h]	2.07
6c	7.48	7.22	7.80 (8.0)	7.22 (8.0)	2.50[d]	5.85[f]	2.07

[a] Broad singlet.
[b] Doublet.
[c] Multiplet.
[d] δ(Ar-Me).
[e] δ(N(1)–Me).
[f] δ(N(1)–CH_2–Ph).
[g] δ(–CH_2–CH_3) quartet for –CH_2–.
[h] Triplet for –CH_3.

Table 5
Selected list of calculated data from TD-DFT excitation energies for **3b** and **5b** in acetonitrile

Excited state	λ, nm($f \times 10^3$)	Major contribution
*Compound **3b***		
1	551.8(10.9)	(79%)HOMO → LUMO (MLCT, IL), (14%)H − 2 → LUMO (IL)
2	512.8(19.2)	(86%)H − 1 → LUMO (MLCT, IL), (10%)H − 2 → LUMO (IL)
3	435.8(358.3)	(49%)H − 2 → LUMO, (18%)H − 4 → LUMO (IL)
5	415(93.7)	(67%)H − 3 → LUMO, (10%)H − 2 → LUMO, (10%)H − 4 → LUMO] (IL)
7	394.7(66.2)	(65%)H − 4 → LUMO, (19%)H − 3 → LUMO] (IL)
*Compound **5b***		
2	528.7(61.2)	(70%)H − 1 → LUMO, (19%)HOMO → LUMO (MLCT, IL)
4	436.7(95.3)	(33%)H − 2 → LUMO, (32%)H − 3 → LUMO, (17%) H − 4 → LUMO (IL)
5	404.2(119.8)	(64%)H − 1 → L + 1, (MLCT, IL), (18%)H − 2 → LUMO (IL)
6	400.4(211.0)	(28%)H − 2 → LUMO, (20%)H − 3 → LUMO, (16%)H − 4 → LUMO (IL), (16%)H − 1 → L + 1 (MLCT, IL)

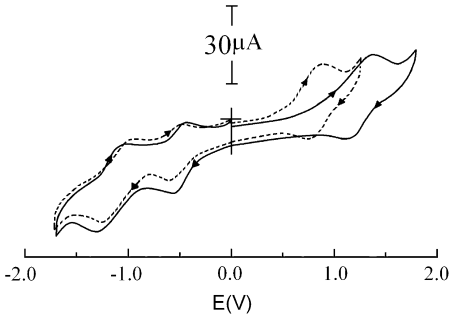

Fig. 5. Cyclic voltammogram of (**3b**) (—) and (**5b**) (– – –) in MeCN using Pt-disk working and Pt-wire auxiliary electrodes and referenced to the Ag/AgCl electrode.

(**3c**); for TaiR: R = Me (**4a**), Et (**4b**), CH_2Ph (**4c**)) has been synthesized by reacting $[Ru(CO)_2Cl_2]_n$ with PaiR or TaiR. The complexes are selectively decarbonylated to isolate *trans*-(Cl)-[$Ru(CO)Cl_2$(PaiR or TaiR)(NCMe)] (**5/6**). However, complete decarbonylation, either by thermal or photochemical methods, has not been possible. The complexes are characterized by spectroscopic data and in one case by an X-ray structure. The computational (DFT) study has discussed the separation of a single isomer on the basis of energy calculation. The electronic structures support metal centered oxidations, and reductions of the chelated ligand.

4. Experimental

4.1. Materials

1-Alkyl-2-(phenylazo)imidazole (**1**) and 1-alkyl-2-(*p*-tolylazo)imidazole (**2**) were synthesized following a previously published procedure [75–81]. $[Ru(CO)_2Cl_2]_n$ was also prepared by the reported method [63,64,76–78]. Imidazole and all other organic chemicals and inorganic salts were available from Sisco Research Lab., Mumbai, India. The purification of acetonitrile and preparation of *n*-tetrabutylammonium perchlorate [nBu$_4$N][ClO_4] for electrochemical work were done as reported before [75–81]. Dinitrogen was purified by bubbling through an alkaline pyrogallol solution. All other chemicals and solvents were of reagent grade and were used without further purification.

4.2. Physical measurements

Microanalytical data (C, H, N) were collected on Perkin–Elmer 2400 CHNS/O elemental analyzer. Spectroscopic data were obtained using the following instruments: UV–Vis spectra, Perkin–Elmer, model Lambda 25; IR spectra (KBr disk, 4000–200 cm^{-1}), Perkin–Elmer, model RX-1; ^{1}H NMR spectra, Bruker (AC) 300 MHz FTNMR spectrometer. Electrochemical measurements were performed using a computer-controlled PAR model 250 VersaStat electrochemical instrument with a Pt-disk electrode. All

Table 6
Summarised crystallographic data for *trans*-(Cl)-[$Ru(CO)_2Cl_2$(PaiEt)](3b)

Empirical formula	$C_{13}H_{12}Cl_2N_4O_2Ru$
Formula weight	428.24
Crystal system	monoclinic
Space group	$P21/c$
a (Å)	10.6772(14)
b (Å)	14.1537(18)
c (Å)	23.074(3)
β (°)	107.173(5)
Size (mm^3)	$0.42 \times 0.19 \times 0.13$
V(Å^3)	3331.5(7)
λ (Å)	0.71073
ρ_{calcd} ($Mg\,m^{-3}$)	1.708
Z	8
T (K)	298(2)
μ(Mo Kα) (mm^{-1})	1.272
Total reflection collected	19700
Unique reflections	6522
Refined parameters	399
Largest difference in peak and hole (e Å^{-3})	0.604 and −0.242
R[a] ($I > 2\sigma(I)$)	0.0330
wR[b]	0.0809
Goodness-of-fit[c]	1.034

[a] $R = \sum||F_o| - |F_c||/\sum|F_o|$.
[b] $wR = [\sum w(F_o^2 - F_c^2)^2/\sum w(F_o^2)^2]^{1/2}$, $w = 1/[s^2(F_o^2) + (0.0417P)^2 + 1.1071P]$, where $P = (F_o^2 + 2F_c^2)/3$.
[c] GOF (Goodness of fit) = $[w(F_o - F_c)/(n_o - n_v)]^{1/2}$, where n_o and n_v denote the number of data and variable.

measurements were carried out under a dinitrogen environment at 298 K with reference to Ag/AgCl in acetonitrile using [nBu_4N][ClO_4] as a supporting electrolyte. The reported potentials are uncorrected for junction potentials.

4.3. Synthesis of trans-(Cl)-[$Ru(CO)_2Cl_2$(PaiEt)] (**3b**)

[$Ru(CO)_2Cl_2$]$_n$ (0.31 g, 1.4 mmol) was dissolved in hot methanol (30 ml). A methanolic solution of PaiEt (0.28 g, 1.4 mmol) was added and the solution was refluxed for 2 h under a dinitrogen atmosphere. The color of the solution changed from orange-red to brown. Under slow evaporation of the solvent, a brown crystalline product was left. The product was further purified from CH2Cl2–MeOH solution. The yield was 0.34 g (58%).

The other complexes were prepared following an identical procedure. The yield varied from 50% to 60%. Microanalytical data: Calc. for $C_{12}H_{10}N_4O_2Cl_2Ru$ (**3a**): C, 34.78; H, 2.41; N, 13.53. Found: C, 34.62; H, 2.38; N, 13.47%. Calc. for $C_{13}H_{12}N_4O_2Cl_2Ru$ (**3b**): C, 36.45; H, 2.80; N, 13.08. Found: C, 36.50; H, 2.81; N, 13.00%. Calc. for $C_{18}H_{14}N_4O_2Cl_2Ru$ (**3c**): C, 44.08; H, 2.86; N, 11.43. Found: C, 43.92; H, 2.81; N, 11.38%. Calc. for $C_{13}H_{12}N_4O_2Cl_2Ru$ (**4a**): C, 36.45; H, 2.80; N, 13.08. Found: C, 36.34; H, 2.78; N, 13.04%. Calc. for $C_{14}H_{14}N_4O_2Cl_2Ru$ (**4b**): C, 38.01; H, 3.17; N, 12.67. Found: C, 37.92; H, 3.23; N, 12.60%. Calc. for $C_{19}H_{16}N_4O_2Cl_2Ru$ (**4c**): C, 45.24; H, 3.17; N, 11.11. Found: C, 45.02; H, 3.21; N, 11.17%.

4.4. Synthesis of trans-(Cl)-[$Ru(CO)Cl_2$(PaiEt)(NCMe)] (5b)

trans-(Cl)-[$Ru(CO)_2Cl_2$(PaiEt)] (**3b**) (0.1 g, 0.24 mmol) was dissolved in dry MeCN and sublimed Me_3NO (0.025 g, 0.33 mmol) was added as a pinch under a dry N_2 environment. The solution was then refluxed for 2 h. The intensity of the bright brown solution was reduced to light brown. The solution was evaporated slowly in air while crystals were deposited on the wall of the beaker. They were collected and dried over a CaCl2 desiccator. These crystals were unstable to X-ray irradiation and we could not perform X-ray diffraction analysis. The yield was 0.087 g (84%).

The other complexes were prepared following an identical procedure. The yield varied from 80% to 90%. Calc. for $C_{13}H_{13}N_5OCl_2Ru$ (**5a**): C, 36.38; H, 2.97; N, 16.30. Found: C, 36.53; H, 3.04; N, 16.39%. Calc. for $C_{14}H_{15}N_5OCl_2Ru$ (**5b**): C, 38.09; H, 3.40; N, 15.87. Found: C, 38.00; H, 3.32; N, 15.83%. Calc. for $C_{19}H_{17}N_5O_2Cl_2$-Ru (**5c**): C, 45.33; H, 3.38; N, 13.92. Found: C, 45.22; H, 3.30; N, 13.98%. Calc. for $C_{14}H_{15}N_5OCl_2Ru$ (**6a**): C, 38.09; H, 3.40; N, 15.87. Found: C, 38.18; H, 3.46; N, 15.82%. Calc. for $C_{15}H_{17}N_5OCl_2Ru$ (**6b**): C, 39.56; H, 3.74; N, 15.38. Found: C, 39.44; H, 3.67; N, 15.30%. Calc. for $C_{20}H_{19}N_5OCl_2Ru$ (**6c**): C, 46.42; H, 3.67; N, 13.54. Found: C, 46.33; H, 3.64; N, 13.48%.

4.5. X-ray crystal structure determination

Crystals of *trans*-(Cl)-[$Ru(CO)_2Cl_2$(PaiEt)] (**3b**) were grown by slow diffusion of a CH_2Cl_2 solution of the complex into hexane. The prismatic red crystal used was of dimensions $0.13 \times 0.19 \times 0.42$ mm. Diffraction data were collected with a Bruker SMART 1 K CCD area-detector diffractometer using fine focused sealed tube graphite-monochromatized Mo Ka radiation (λ = 0.7107 Å). A summary of the crystallographic data and structure refinement parameters are given in Table 6. Data were corrected for Lorentz and polarization effects. Data reduction was carried out using the 'Bruker SAINT' program. The structure was solved by direct methods using SHELXS-97 [82] and successive difference Fourier syntheses. All non-hydrogen atoms were refined anisotropically. Full matrix least squares refinements on F_0^2 were carried out using SHELXL-97 [83] with anisotropic displacement parameters for all non-hydrogen atoms. Hydrogen atoms were constrained to ride on the respective carbon or nitrogen atoms with isotropic displacement parameters equal to 1.2 times the equivalent isotropic displacement of their parent atom in all cases. All calculations were carried out using SHELXS 97 [82] and PLATON 99 [84] programs.

5. Supplementary data

CCDC 645194 contains the supplementary crystallographic data for [$Ru(CO)_2Cl_2$(PaiEt)] (**3b**). These data can be obtained free of charge via http://www.ccdc.cam.ac.uk/conts/retrieving.html, or from the Cambridge Crystallographic Data Centre, 12 Union Road, Cambridge CB2 1EZ, UK; fax: (+44) 1223-336-033; or e-mail: deposit@ccdc.cam.ac.uk.

Acknowledgements

Financial support from DST and UGC, New Delhi are thankfully acknowledged. We thank Dr. A.D. Jana for crystallographic graphics.

References

[1] J. Reedijk, in: G. Willkinson, J.A. Mccleverty (Eds.), Comprehensive Coordination Chemistry, vol. 2, Pergamon, Oxford, UK, 1987, p. 430.
[2] W.T. Wong, Coord. Chem. Rev. 131 (1994) 45.
[3] G. Wilkinson, F.G.A. Stone, E.W. Abel (Eds.), Comprehensive Organometallic Chemistry, Pergamon Press, New York, 1982.
[4] F.A. Cotton, G. Wilkinson, Advanced Inorganic Chemistry, 5th ed., Wiley-Interscience, New York, 1994.
[5] K. Kalyansundaram, Coord. Chem. Rev. 46 (1982) 159.
[6] B.K. Ghosh, A. Chakravorty, Coord. Chem. Rev. 95 (1989) 239.
[7] N. Bag, A. Pramanik, G.K. Lahiri, A. Chakravorty, Inorg. Chem. 31 (1992) 40.
[8] S. Serroni, S. Campagna, F. Puntoriero, C.D. Pietro, N.D. Mcclenaghan, F. Loisean, Chem. Soc. Rev. 30 (2001) 367.
[9] A.C.G. Hotze, H. Kooijman, A.L. Spek, J.G. Haasnoot, J. Reedijk, New J. Chem. 28 (2004) 565.
[10] R.E. Shepherd, Coord. Chem. Rev. 247 (2002) 147.
[11] M.J. Overett, J.R. Moss, Inorg. Chim. Acta 358 (2005) 1715.
[12] S.J. Dougan, M. Melchart, A. Habtemariam, S. Parsons, P.J. Sadler, Inorg. Chem. 45 (2006) 10882.
[13] C.K. Pal, S. Chattopadhyay, C. Sinha, D. Bandhyopadhyay, A. Chakravorty, Polyhedron 13 (1994) 999.
[14] P.K. Santra, R. Roy, C. Sinha, Proc. Indian Acad. Sci. (Chem. Sci.) 112 (2000) 523.
[15] B.K. Santra, P. Munshi, G. Das, P. Bharadwaj, G.K. Lahiri, Polyhedron 18 (1999) 617.
[16] P.K. Santra, P. Byabratta, S. Chattopadhyay, C. Sinha, L.R. Falvello, Eur. J. Inorg. Chem. (2002) 1124.
[17] M. Panda, S. Das, G. Mostafa, A. Castineiras, S. Goswami, J Chem. Soc., Dalton Trans. (2005) 1249.
[18] U.S. Ray, B.K. Ghosh, M. Monfort, J. Ribas, G. Mostafa, T.-H. Lu, C. Sinha, Eur. J. Inorg. Chem. (2004) 250.
[19] U.S. Ray, B.G. Chand, G. Mostafa, J. Cheng, T.-H. Lu, C. Sinha, Polyhedron 22 (2003) 2587.
[20] D. Banerjee, U.S. Ray, J.-C. Liou, C.-N. Lin, T.-H. Lu, C. Sinha, Inorg. Chim. Acta 358 (2005) 1019.
[21] U.S. Ray, D. Banerjee, B.G. Chand, J. Cheng, T. –H. Lu, C. Sinha, J. Coord. Chem. 58 (2005) 1105.
[22] B.G. Chand, U.S. Ray, J. Cheng, T.-H. Lu, C. Sinha, Polyhedron 22 (2003) 1213.
[23] B.G. Chand, U.S. Ray, G. Mostafa, T.-H. Lu, C. Sinha, Polyhedron 23 (2004) 1669.
[24] B.G. Chand, U.S. Ray, G. Mostafa, T.-H. Lu, C. Sinha, J. Coord. Chem. 57 (2004) 627.
[25] B.G. Chand, U.S. Ray, J. Cheng, T.-H. Lu, C. Sinha, Inorg. Chim. Acta 358 (2005) 1927.
[26] T.K. Misra, D. Das, C. Sinha, P.K. Ghosh, C.K. Pal, Inorg. Chem. 37 (1998) 1672.
[27] T.K. Misra, D. Das, C. Sinha, Polyhedron 16 (1997) 4163.
[28] T.K. Misra, D. Das, C. Sinha, Indian J. Chem. A 37 (1998) 741.
[29] S. Pal, T.K. Misra, P. Chattopadhyay, C. Sinha, Proc. Indian Acad. Sci. (Chem. Sci.) 111 (1999) 687.
[30] M.N. Ackermann, C.R. Barton, C.J. Deodene, E.M. Specht, S.C. Keill, W.E. Schreiber, Hiodong. Kim, Inorg. Chem. 28 (1989) 397.
[31] F. Alper, C. Kayram, S. Ozkar, J. Organomet. Chem. 691 (2006) 2734.
[32] W. Kaim, S. Ernst, S. Kohlmann, Polyhedron 5 (1986) 295.
[33] W. Kaim, S. Kohlmann, Inorg. Chem. 25 (1986) 3442.
[34] W. Kaim, S. Kohlmann, Inorg. Chem. 26 (1987) 68.
[35] M.N. Ackermann, W.G. Fairbrother, N.S. Amin, C.J. Deodene, C.M. Lamborg, P.T. Martin, J. Organomet. Chem. 523 (1996) 145.
[36] M.J. Alder, W.I. Cross, K.R. Flower, R.G. Pritchard, J. Organomet. Chem. 568 (1998) 279.
[37] M.N. Ackermann, S.R. Kiihne, P.A. Saunders, C.E. Barnes, S.C. Stalling, H. Kim, C. Woods, M. Lagunoff, Inorg. Chim. Acta 334 (2002) 193.
[38] M.N. Ackermann, M.P. Robinson, I.A. Maher, E.B. LeBlane, R.V. Raz, J. Organomet. Chem. 682 (2003) 248.
[39] P. Datta, P. Gayen, C. Sinha, Polyhedron 25 (2006) 3435.
[40] M.A. Moreno, M. Haukka, A. Turunen, T.A. Pakkanen, J. Mol. Catal. A: Chem. 240 (2005) 7.
[41] E.A. Seddon, K.R. Seddon, The Chemistry of Ruthenium;, Elsevier, Amsterdam, 1984.
[42] S. Goswami, A.R. Chakravarty, A. Chakravorty, Inorg. Chem. 20 (1981) 2246. 21 (1982) 2173; 22 (1983) 602.
[43] S. Goswami, R.N. Mukherjee, A. Chakravorty, Inorg. Chem. 22 (1983) 2825.
[44] P. Ghosh, A. Chakravorty, J. Chem. Soc., Dalton Trans. (1985) 361.
[45] G.K. Lahiri, S. Bhattacharya, S. Goswami, A. Chakravorty, J. Chem. Soc., Dalton Trans. (1990) 561.
[46] G.K. Lahiri, S. Goswami, L.R. Falvello, A. Chakravorty, Inorg. Chem. 26 (1987) 3365.
[47] R. Samanta, P. Munshi, B.K. Santra, N.K. Loknath, M.A. Sridhar, J.S. Prasad, G.K. Lahiri, J. Org. Met. Chem. 579 (1999) 311.
[48] R.A. Krause, K. Krause, Inorg. Chem. 19 (1980) 2600. 1982 (21) 1714; 1984 (23) 219.
[49] A. Bharat, B.K. Santra, P. Munshi, G.K. Lahiri, J. Chem. Soc., Dalton Trans. (1998) 2643.
[50] A. Seal, S. Roy, Acta Crystallogr., Sect C C40 (1984) 929.
[51] A.H. Velders, H. Kooijman, A.L. Spek, J.G. Haasnoot, D. de Vos, J. Reedijk, Inorg. Chem. 39 (2000) 2966.
[52] A.C.G. Hotze, A.H. Velders, F. Ugozzoli, M. Bicingi, A.M. Manotti-Lanfredi, J.G. Haasnoot, J. Reedijk, Inorg. Chem. 39 (2000) 3838.
[53] M. Shivakumar, K. Pramanik, P. Ghosh, A. Chakravorty, Chem. Commun. (1998) 2103.
[54] K.S.Y. Leung, Y. Li, Inorg. Chem. Commun. 2 (1999) 599.
[55] W.Y. Wong, S.H. Cheung, S.M. Lee, S.Y. Leung, J. Org. Chem. 596 (2000) 36.
[56] K. Pramanik, M. Shivakumar, P. Ghosh, A. Chakravorty, Inorg. Chem. 39 (2000) 195.
[57] V.W.W. Yam, V.C.Y. Lan, L.X. Wu, J. Chem. Soc., Dalton Trans. (1998) 1461.
[58] R. Samanta, P. Munshi, B.K. Santra, N.K. Loknath, M.A. Sridhar, J.S. Prasad, G.K. Lahiri, J. Organomet. Chem. 579 (1999) 311.
[59] G. Cripps, A. Pellissier, S. Chardon-Noblat, A. Deronzier, R.J. Haines, J. Organomet. Chem. 689 (2004) 484.
[60] S. Chardon-Noblat, A. Deronzier, R. Ziessel, D. Zsoldos, J. Electroanal. Chem. 444 (1998) 253.
[61] J.-M. Lehn, R. Ziessel, J. Organomet. Chem. 382 (1990) 157.
[62] S. Chardon-Noblat, A. Deronzier, R. Ziessel, Collect. Czech. Chem. Commun. 66 (2001) 207.
[63] J.M. Kelly, C.M. O_Connell, J.G. Vos, Inorg. Chim. Acta 64 (1982) L75.
[64] S. Chardon-Noblat, P. Da Costa, A. Deronzier, M. Haukka, T.A. Pakkanen, R. Ziessel, J. Electroanal. Chem. 490 (2000) 62.
[65] H. Sigel (Ed.), Metal Ions in Biological System, vol. 13, Marcel Dekker, New York, 1981.
[66] J. Otsuki, K. Suwa, K. Narutaki, C. Sinha, I. Yoshikawa, K. Araki, J. Phys. Chem. A 109 (2005) 8064.
[67] J. Otsuki, K. Suwa, K.K. Sarker, C. Sinha, J. Phys. Chem. A 111 (8) (2007) 1403.
[68] P. Bhunia, B. Baruri, U.S. Ray, C. Sinha, S. Das, J. Cheng, T.-H. Lu, Transition Met. Chem. 31 (2006) 310.
[69] E.Y. Li, Y.-M. Cheng, C.-C. Hsu, P.-T. Chou, G.-S. Lee, I.-H. Lin, Y. Chi, C.-S. Liu, Inorg. Chem. 45 (2006) 8041.
[70] E. Eskelinen, M. Haukka, T. Venalainen, T.A. Pakkanen, M. Wasberg, S. Chardon-Noblat, A. Deronzier, Organometallics 19 (2000) 163.
[71] M.J. Frisch, G.W. Trucks, H.B. Schlegel, P.M.W. Gill, B.G. Johnson, M.A. Robb, J.R. Cheeseman, T.A. Keith, G.A. Petersson, J.A. Montgomery, K. Raghavachari, M.A. Al-Laham, V.G. Zakrzewski, J.V. Ortiz, J.B. Foresman, J. Cioslowski, B.B. Stefanov, A. Nanayakkara, M. Challacombe, C.Y. Peng, P.Y. Ayala, W. Chen, M.W. Wong, J.L. Andres, E.S. Replogle, R. Gomperts, R.L. Martin, D.J. Fox, J.S. Binkley, D.J. Defrees, J. Baker, J.P. Stewart, M. Head-Gordon, C. Gonzalez, J.A. Pople, GAUSSIAN98, Gaussian, Inc., Pittsburgh, PA, 1998.
[72] C. Lee, W. Yang, R.G. Parr, Phys. Rev. B 37 (1988) 785.
[73] P.J. Hay, W.R. Wadt, J. Chem. Phys. 82 (1985) 270.
[74] M. Cossi, V.J. Barone, Chem. Phys. 115 (2001) 4708.
[75] N.M. O'Boyle, J.G. Vos, GaussSum 1.0, Dublin City University, Dublin, Ireland, 2005. <http://www.gausssum.sourceforge.net>.
[76] M.I. Bruce, Ruthenium carbonyls and related compounds, in: G. Wilkinson, F.G.A. Stone, E.W. Abel (Eds.), Comprehensive Organometallic Chemistry, vol. 4, Pergamon Press, Oxford, 1982, p. 661.
[77] A.J. Deeming, C. Forth, G. Hogarth, Transition Met. Chem. 31 (2006) 42.
[78] M. Haukka, J. Kiviaho, M. Ahlgren, T.A. Pakkam, Organometallics 14 (1995) 825.
[79] J. Dinda, Ph.D. Thesis, The University of Burdwan, Burdwan, India, 2003.
[80] J. Dinda, K. Bag, C. Sinha, G. Mostafa, T.-H. Lu, Polyhedron 22 (2003) 1367.
[81] A. Gabrielsson, S. Zalis, P. Matousek, M. Towrie, A. Vlcek Jr., Inorg. Chem. 43 (2004) 7380.
[82] G.M. Sheldrick, SHELXS-97, Program for the Solution of Crystal Structure, University of Gottingen, Germany, 1997.
[83] G.M. Sheldrick, SHELXL-97, Program for the Solution of Crystal Structure, University of Gottingen, Germany, 1997.
[84] A.L. Spek, PLATON, Molecular Geometry Program, University of Utrecht, The Netherlands, 1999.